Response of Gravity Level Fluctuations on the Gravity Probe-B Spacecraft Propellant System

R. J. Hung* and C. C. Lee†
University of Alabama in Huntsville, Huntsville, Alabama 35899
and
F. W. Leslie‡
NASA Marshall Space Flight Center, Huntsville, Alabama 35812

The dynamical behavior of fluids, in particular, the effect of surface tension on partially filled fluids in a rotating dewar under microgravity environment, has been investigated. Results show that there is a group of wave trains, both in longitudinal and transverse modes, with various frequencies and wavelengths of slosh waves generated by the restoring force field of gravity jitters and centrifugal forces in this study. The longest wave periods of slosh waves, either the longitudinal or transverse modes, are responsible for the production of wave modes with the highest ratio of maximum wave amplitude to wavelength. Also, the lower frequency slosh waves are the wave modes with higher wave energy than that of the higher frequency slosh waves.

Nomenclature

a	=	radius of the circular cylinder
f_o	=	frequency of gravity jitters, defined by Eq. (13)
g	=	gravitational acceleration
g_B	=	background gravity environment, defined by Eq. (13)
g_0	=	normal Earth gravitational acceleration, 9.81 m/s^2
L	=	length of the cylinder
$Max(A/\lambda)$	=	ratio of maximum wave amplitude to wavelength
n	=	unit vector normal to the interface
P	=	pressure
r	=	cylindrical coordinate along radial direction
t	=	time
u	=	velocity component along radial direction
v	=	velocity component along axial direction
z	=	cylindrical coordinate along axial direction
δ	=	Dirac delta function
ζ	=	viscous coefficient of the second kind
η	=	profile of interface between gaseous and liquid fluids, defined by Eq. (7)
θ	=	cylindrical coordinate along circumferential direction
μ	=	viscous coefficient of the first kind
ν	=	kinematic viscosity coefficient
ρ	=	density
σ	=	surface tension of the interface
τ_{ij}	=	viscous stress tensor
ϕ	=	tangent of interface, defined by Eq. (12)
ω	=	rotating angular velocity of cylinder

Subscripts

G	=	gaseous fluid
L	=	liquid fluid

Received July 10, 1989; revision received May 23, 1990; accepted for publication June 27, 1990.

*Professor, Department of Mechanical Engineering. Associate Fellow AIAA.
†Research Engineer, Department of Mechanical Engineering.
‡Chief, Fluid Dynamics Branch.

Introduction

THE Gravity Probe-B (GP-B) Spacecraft (see Fig. 1) is designed to test the general theory of relativity through a long-term (1 year) monitoring of the procession of a set of gyros in free-fall around the Earth.[1,2] Extraneous forces on these gyros must be kept at very low levels, corresponding to an acceleration of 10^{-10} g_0 (g_0 = 9.81 m/s^2) or less. This will require a drag-free (to 10^{-10} g_0) control system using a proof mass similar to the experiment gyros as its sensing element. The experiment uses superconducting sensors for gyro readout and maintains very low temperature for mechanical stability. The approaches to both cooling and control involve the use of superfluid liquid helium. The boil-off from the liquid helium dewar (Fig. 2) will be used as a propellant to maintain the attitude control and drag-free operation of the spacecraft. The requirement for an operational lifetime approaching one year means that a large quantity of liquid helium must be used, and that it will be gradually depleted over the lifetime of the experiment. This varying amount of liquid helium gives rise to the possibility of several problems that could degrade the GP-B experiment. The potential problems could be due to asymmetry in the static liquid helium distribution or to perturbations in the free surface.

In a study of the attraction of unsymmetric liquid helium distributions on the proof mass, Schafer and Lowry[3] showed that, with liquid helium on one side in a half-full dewar, the resulting acceleration levels at the proof mass are about 10^{-8} g_0. In the absence of temperature gradient along the

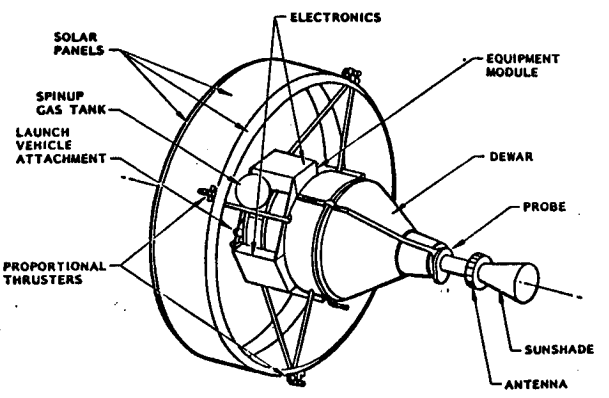

Fig. 1 Gravity Probe-B Spacecraft conceptual design.

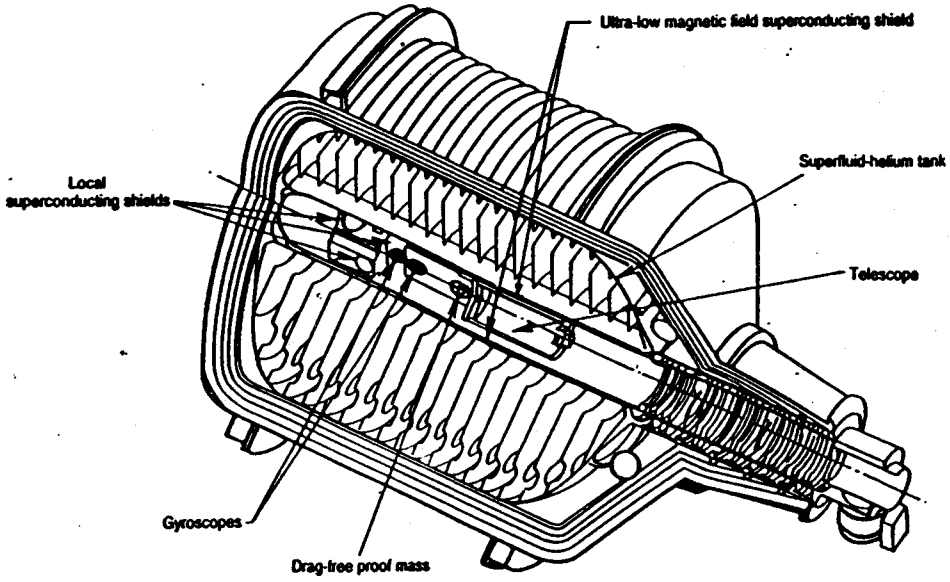

Fig. 2 The experiment GP-B module showing main elements of the liquid helium dewar and probe.

surface driving the Marangoni convection, the equilibrium shape of a free surface is governed by a balance of capillary, centrifugal, and gravitational forces. In contrasting the effects of surface tension to the effects of gravitational forces on the free surface of liquid, it was found that the surface tension force for most liquids is greater than the gravitational force in a 10^{-8} g_0 level and lower.[4–6] In other words, the equilibrium shape of the liquid helium free surface in the operational GP-B Spacecraft is governed by a balance of capillary and centrifugal forces, instead of a balance of capillary, centrifugal, and gravitational forces. Therefore, one may ignore the effect of gravitational force in the gravity environment levels of 10^{-8} g_0 and lower in comparison to the surface tension force. Determination of bubble profiles based on computational experiments can uncover details of the flow that cannot easily be visualized or measured experimentally.[7–10]

Surface tension plays an important role in a large variety of fluid flows. The equilibrium shape of the free surface for the unsteady state rotating fluids is governed by the balance of capillary, bulk pressure, viscous, centrifugal, and gravity forces. The configuration of interface between liquid and gaseous fluids will be modified greatly when the gravity field reduces to microgravity levels. The instability of liquid surface can be induced by the presence of longitudinal and lateral accelerations, vehicle vibration, and rotational fields of spacecraft in a microgravity environment. Slosh waves are, thus, excited that produce high- and low-frequency oscillations in the liquid propellant. The sources of the residual accelerations range from the effects of the Earth's gravity gradient, atmospheric drag on the spacecraft, and spacecraft attitude motions to the higher frequency "g-jitter" arising from machinery vibrations, thruster firings, and crew motions. Recent study[11] suggests that the high-frequency accelerations may be unimportant in comparison to the residual motions caused by low-frequency accelerations.

Behavior of the liquid propellant becomes uncertain when the gravity environment is reduced on the order of 10^{-6} g_0 level. The requirement to settle or to position liquid fuel over the outlet end of the spacecraft propellant tank prior to main engine restart poses a microgravity fluid behavior problem. Retromaneuvers of spacecraft, such as the Orbital Maneuvering Vehicle (OMV) and Space Transfer Vehicle (STV)[12] during flight from high earth orbit to low earth orbit, require settling or reorientation of the propellant prior to main engine firing. Cryogenic liquid propellant is positioned over the tank outlet by using small auxiliary thrusters (or an idle-mode thruster from the main engine) that provide a thrust parallel to the tank's major axis in the direction of flight.[13]

Time-dependent dynamical behavior of surface tension on partially filled rotating fluids in both low-gravity and microgravity environments was carried out by numerically computing the Navier-Stokes equations subjected to the initial and boundary conditions.[6,14] At the interface between the liquid and the gaseous fluids, both the kinematic surface boundary condition and the interface stress conditions for components tangential and normal to the interface were applied. The initial condition of bubble profiles was adopted from the steady-state formulations, in which the computer algorithms have been developed by Hung and Leslie,[4] and Hung et al.[5] in a rotating cylinder tank, and, also, by Hung et al.[5,15] in the coordinate of the GP-B Spacecraft.[2] Some of the steady-state formulations of bubble shapes, in particular, for bubbles intersecting the top wall of the cylinder, were compared with the available experiments carried out by Leslie[7] in a free-falling aircraft (KC-135). In the KC-135 experiments, the background gravity varies from 1.8 to 10^{-2} g_0 in about 40 s. It is difficult to calibrate the recording of corresponding time-dependent gravity variations of the dynamical evolution of bubble profiles in a very short period of observations under microgravity environment. Furthermore, a very sensitive and high-degree of accuracy accelerometer for measuring the levels of microgravity is unavailable, which makes the comparisons of time-dependent results between numerical computations and experiments unavailable at this time.

For the GP-B Spacecraft liquid helium management problem, the geometries are so large that the critical values of superfluid are exceeded. The experiments carried out by Mason et al.[16] showed that the classical fluid mechanics theory is applicable for liquid helium in large containers.[17]

The equilibrium configurations of the helium bubble in a rotating dewar was studied.[5] They are relevant to the questions of fluid behavior in a microgravity environment raised by design and operational considerations for the GP-B experiment. For a spacecraft operating as designed, spacecraft drag will be balanced by the helium propulsion system. There should be no net acceleration, above the 10^{-10} g_0 level, on the liquid helium from these sources. Our earlier studies[4–6] showed that the gravitational force of 10^{-8} g_0 level and lower will never affect the equilibrium shape of the liquid helium free surface, because the effect of the surface tension force is overwhelmingly greater than that of the gravitational force at these levels.

As to the effect of centrifugal force on the helium bubble, the dewar will not be spinning when the GP-B spacecraft is deployed. In the early stages of the experiment, a spin rate of up to about 1 rpm will be imposed for instrument calibration. After calibration, the rotation rate will be reduced to its operational value of approximately 0.1 rpm.

In this study, time-dependent computations have been carried out to investigate the dynamical behaviors of fluid under a microgravity environment. The computation extends to the study of sloshing waves induced by the g-jitters, and variations in rotation speeds of dewar and background gravity fields.

Mathematical Formulation

Consider a closed circular cylinder of radius a with length L partially filled with a Newtonian fluid of constant density ρ and kinematic viscosity ν. The cylinder rotates about its axis of symmetry with angular velocity, $\omega(t)$, which is a function of time t.

Let us use cylindrical coordinates (r, θ, z) with corresponding velocity components (u, v, w). The gravitational acceleration g, is along the z-axis. For the case of axial symmetry, the θ-dependency vanishes. The governing equations are shown as follows:

Continuity equation

$$\frac{1}{r}\frac{\partial}{\partial r}(ru) + \frac{\partial w}{\partial z} = 0 \tag{1}$$

Momentum equations

$$\frac{Du}{Dt} - \frac{v^2}{r} = -\frac{1}{\rho}\frac{\partial P}{\partial r} + \nu\left(\nabla^2 u - \frac{u}{r^2}\right) \tag{2}$$

$$\frac{Dv}{Dt} + \frac{uv}{r} = \nu\left(\nabla^2 v - \frac{v}{r^2}\right) \tag{3}$$

$$\frac{Dw}{Dt} = -\frac{1}{\rho}\frac{\partial P}{\partial z} - g + \nu\nabla^2 w \tag{4}$$

where

$$\frac{D}{Dt} = \frac{\partial}{\partial t} + u\frac{\partial}{\partial r} + w\frac{\partial}{\partial z} \tag{5}$$

$$\nabla^2 = \frac{1}{r}\frac{\partial}{\partial r}\left(r\frac{\partial}{\partial r}\right) + \frac{\partial^2}{\partial z^2} \tag{6}$$

Let the profile of the interface between gaseous and liquid fluids be given by

$$\eta(t, r, z) = 0, \text{ or } r = \eta(t, z) \tag{7}$$

The initial condition of the profile of interface between gaseous and liquid fluids at $t = t_o$ is assigned explicitly, and is given by

$$\eta(t = t_o, r, z) = 0, \text{ or } r = \eta_0(z) = \eta(t_o, z) \tag{8}$$

A set of boundary conditions has to be supplied for solving the equations. These initial interface profiles used in this study have been given explicitly through the steady-state computations made by Hung and Leslie[4] and Hung et al.,[5,6] which were checked by the experiments carried over by Leslie.[7] These boundary conditions are as follows:

1) At the container wall, no-penetration and no-slip conditions assure that both the tangential and the normal components of the velocity along the solid walls will vanish. In the numerical calculation of bubble profiles for liquid and air, a constant contact angle is present when the free surface of liquid intersects the container wall.

2) Along the interface between the liquid and gaseous fluids, the following two conditions apply:

a) Kinematic surface boundary condition: The liquid (or gaseous) surface moves with the liquid (or gas) which implies

$$\frac{D\eta}{Dt} = 0, \qquad \text{or}$$

$$\frac{\partial \eta}{\partial t} + u\frac{\partial \eta}{\partial r} + w\frac{\partial \eta}{\partial z} = 0$$

$$\text{on} \quad \eta = \eta(t = t_i, r, z) \tag{9}$$

b) Interface stress condition: At the interface, the stress must be continuous. These can be decomposed to the components normal and tangential to the interface. For the component tangential to the interface between liquid and gaseous fluids

$$[\underset{\sim}{\tau} \cdot \underset{\sim}{n} - (\underset{\sim}{n} \cdot \underset{\sim}{\tau} \cdot \underset{\sim}{n})]_{\text{liquid}} = [\underset{\sim}{\tau} \cdot \underset{\sim}{n} - (\underset{\sim}{n} \cdot \underset{\sim}{\tau} \cdot \underset{\sim}{n})]_{\text{gas}} \tag{10}$$

must hold. Here

$$\tau_{ij} = \mu\left(\frac{\partial u_i}{\partial x_j} + \frac{\partial u_j}{\partial x_i} + \frac{2}{3}\frac{\partial u_k}{\partial x_k}\delta_{ij}\right) + \zeta\frac{\partial u_k}{\partial x_k}\delta_{ij}$$

is the viscous stress tensor; μ, the viscous coefficient of the first kind; ζ, the viscous coefficient of the second kind; $\underset{\sim}{n}$, the unit vector normal to the interface, δ_{ij}, the Dirac delta function. For the component normal to the interface between the liquid and gaseous fluids, the expression becomes Laplace's formula, which is

$$P_G - P_L - (\underset{\sim}{n} \cdot \underset{\sim}{\tau} \cdot \underset{\sim}{n})_{\text{gas}} + (\underset{\sim}{n} \cdot \underset{\sim}{\tau} \cdot \underset{\sim}{n})_{\text{liquid}} = -\frac{\sigma}{r}\frac{\mathrm{d}}{\mathrm{d}r}\left[\frac{r\phi}{(1 + \phi^2)^{1/2}}\right] \tag{11}$$

Here, P_L denotes the liquid pressure at the interface; P_G, the gaseous pressure at the interface; σ, the surface tension of the interface; ϕ, the tangent of the interface, defined by

$$\phi = \frac{\mathrm{d}z}{\mathrm{d}r} \text{ on } \eta_i = \eta(t_i, r, z) \tag{12}$$

Numerical Simulation of Fluid Behaviors in Rotating Dewar Under Microgravity Environments

The present study examined time-dependent fluid behaviors, in particular the dynamics of the liquid helium and helium vapor in rotating dewar under microgravity environments. In other words, the initial bubble profiles computed from the steady-state formulation, in conjuction with the following parameters, such as liquid density (ρ_L) and its kinematic viscosity (ν_L); gas density (ρ_G) and its kinematic viscosity (ν_G); surface tension coefficient (σ), angular velocity (ω), and gravity environment (g), etc., used as the initial input for the time-dependent computation. Thus, the initial condition of the interface profile between gaseous and liquid fluids at $t = t_o$ can be assigned explicitly with Eq. (8).

A staggered grid for the velocity components is used in this computer program that was first developed by Harlow and Welch[18] in their Marker and Cell (MAC) method to study fluid flows with free surface. Figure 3 shows a three-dimensional schematic expression of the distribution of grid points in cylindrical coordinates. Also, it shows staggered locations in the r-z plane in which $\rightarrow$ denotes staggered locations for the radial component of velocity u; $\uparrow$, for the axial component of velocity w; and o, for other variables such as pressure.

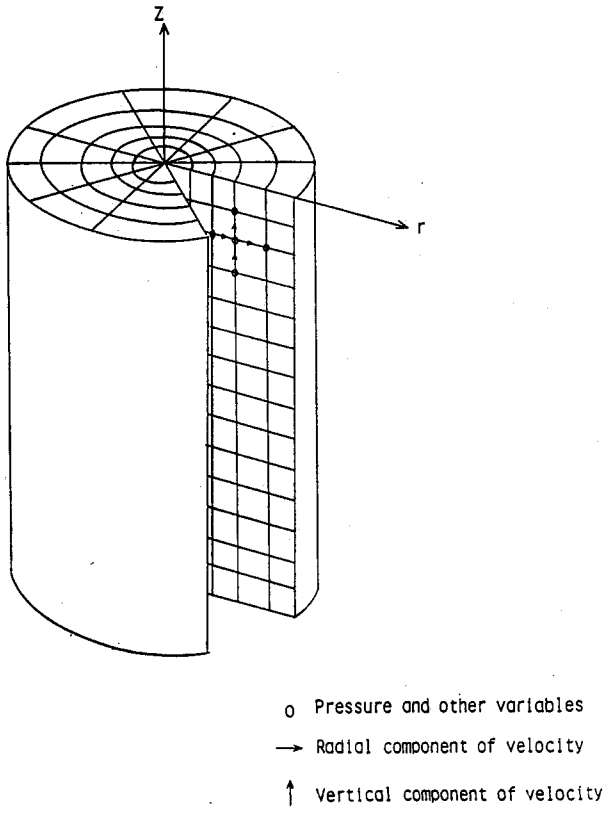

Fig. 3 Three-dimensional schematic expression of the distribution of grid points in cylindrical coordinates. Also, staggered location in the *r-z* plane in which → denotes staggered location for the radial component of velocity; ↑, for the axial component of velocity; and *o*, for other variables, such as pressure.

The finite-difference scheme employed in this numerical study was the hybrid scheme developed by Spalding.[19] The formulation for this scheme is valid for any arbitrary interface location between the grid points, and is not limited to midway interfaces.[20] An algorithm of the semi-implicit method[21] was used as the procedure for developing the calculation of the flowfield. The time step is determined automatically, based on the size of the grid points and the angular velocity of rotating fluids.

A computer algorithm was developed to integrate Eqs. (1–4) numerically, subjected to the following conditions: 1) initial condition, Eq. (8); 2) boundary conditions that include no-penetration and no-slip conditions at the container wall; 3) kinematic surface boundary condition, shown in Eq. (9); and 4) interface stress conditions, shown in Eqs. (10–12).

The present study examines the characteristics of slosh waves excited by the gravity jitters under different background gravity fields and different speeds of rotating dewar with the GP-B spacecraft geometry. Transport coefficients of normal liquid helium and helium vapor at 4 K are used, since experimental results[16] show that they have exceeded the critical values of superfluid for the large geometries to be used in the GP-B Spacecraft propulsion system.[17] In this study, the following data was used: liquid helium density = 0.145 g/cm^3, helium vapor density = 0.00147 g/cm^3, surface tension between vapor and liquid helium = 0.5 dyne/cm, temperature of liquid helium = 4 K. Computation is based on 90% liquid helium and 10% helium vapor by volume contained in the dewar. The contact angles between liquid helium and the solid walls for all the cases are $\theta = 10°$. The size of the dewar is as follows: outer radius = 68 cm, inner radius = 12 cm, and height = 145 cm. The frequency of gravity jitters is defined through the vibration of gravity environment, which is governed by the following formula:

$$g = g_B \left[1 + \frac{1}{2} \sin (2\pi f_o t)\right] \tag{13}$$

where g_B denotes the background gravity environment, and f_o (Hz) stands for the vibration frequency of gravity jitters.

Excitation of Slosh Waves due to Gravity Jitters at Different Background Gravity Levels

Evolution of slosh waves caused by the gravity jitters and centrifugal forces has been investigated. The frequency of gravity jitters is 1.0 Hz; the rotating speed of dewar is 0.1 rpm; and different background gravity levels at 10^{-4} and 10^{-5} g_0 are considered.

Figures 4a–4d show the evolution of slosh waves caused by gravity-jitters with frequency of 1.0 Hz at the background gravity environment of 10^{-4} g_0. Top portions of the Figs. 4a and 4b illustrate the vibrations of gravity environment with respect to time, and also the variations of gravity-jitter frequency with respect to time. Figs. 4a–4f show time sequences of evolution for slosh waves from $t = 0.0$ to 3.62 s. It shows clearly a series of slosh wave oscillations caused by the gravity jitters and centrifugal force for partially filled cryogenic helium in a rotating dewar. Figure 5 shows the time series of wave amplitudes for interface fluctuations at $y_1 = 127.0$, $y_2 = 128.9$, and $y_3 = 138.4$ cm in the vertical coordinate, measured from the bottom of a rotating dewar.

The wave period of various modes of slosh waves can be determined from the Fourier power spectral analysis of time series at y_1, y_2, and y_3, whereas wavelength, phase velocity, and propagation direction of slosh waves can be deduced from the cross-correlation analysis of the combinations of any two time series selected out of the three time series.[22–25] Figure

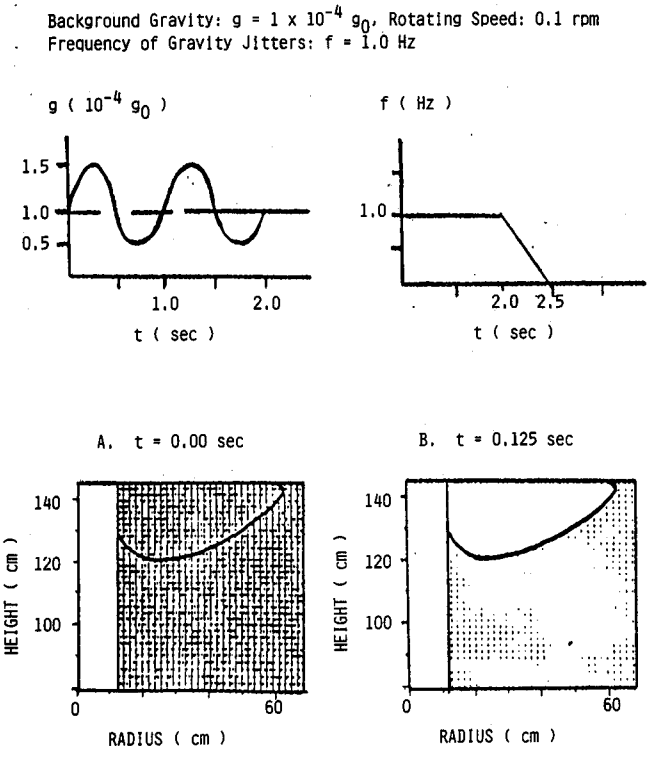

Figs. 4a and 4b Time sequence evolutions of interface between liquid helium and helium vapor in a rotating dewar ($\omega = 0.1$ rpm) with a background gravity of 10^{-4} g_0, subjected to the vibration of gravity jitters with a frequency of 1.0 Hz. Top figures illustrate time-dependent variations of gravity environment and that of the frequency of gravity jitters. Figures 4a shows the profiles of interface at $t = 0.0$ s, and Fig. 4b at $t = 0.125$ s.

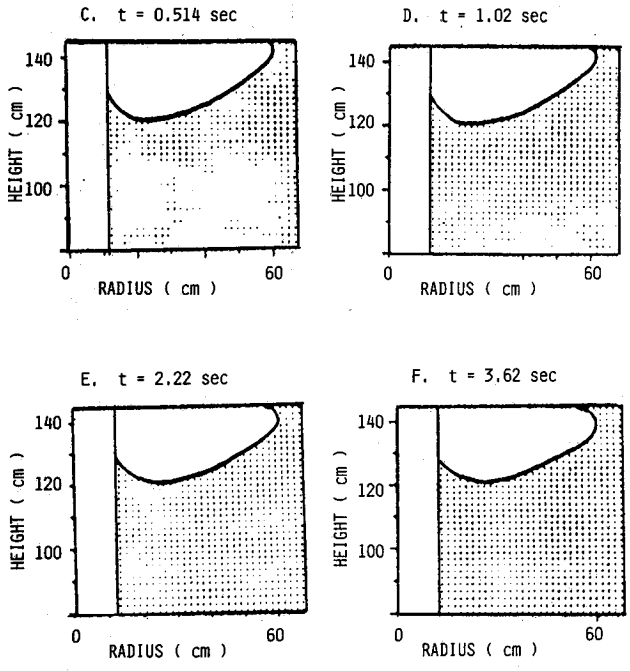

Figs. 4c–4f Time sequence evolutions of interface between liquid helium and helium vapor in a rotating dewar (ω = 0.1 rpm) with a background gravity of 10^{-4} g_0, subjected to the vibration of gravity jitters with a frequency of 1.0 Hz. Figure 4c shows the profiles of interface at t = 0.514 s, Fig. 4d at t = 1.02 s, Fig. 4e at t = 2.22 s and Fig. 4f at t = 3.62 s.

6 shows a sample Fourier power spectral analysis of time series at y_1. This figure clearly indicates that there are five major peaks of wave nodes corresponding to wave periods of 0.59, 0.83, 1.03, 1.28, and 1.46 s. A filter shall be properly chosen by applying certain ranges of window for separating each wave mode out of five wave nodes contained in three time series at y_1, y_2, and y_3, shown in Figure 7 for the determination of wavelength, phase velocity, and propagation direction of slosh waves.[22–25]

Table 1 shows the characteristics of major slosh waves induced by the restoring force field of gravity jitters. Analysis shows that there are one longitudinal mode and four transverse modes detected in this case. Existence of a transverse mode was not detected for slosh waves induced by the restoring force field of gravity jitters in a plain rotating cylindrical container.[26] In other words, the geometry of the rotating dewar (a cylindrical container with a solid core aligned along rotating axis) is responsible for the initiation of transverse modes induced by the restoring force field of gravity jitters combined with centrifugal forces. Propagation direction is measured clockwise from a positive axial direction. Ratio of maximum wave amplitude to wavelength [$Max(A/\lambda)$ ratio, where A is wave amplitude and λ denotes wavelength] for each slosh wave is calculated, using the following procedures:

1) Determine each major wave mode, based on the peaks of power intensity shown in the power spectral density analysis in the Fourier domain (see Fig. 6).

2) Apply proper window of filter to separate each wave mode from a series of wave modes shown on the peaks of power intensity.

3) Calculate wavelength, phase velocity, and propagation direction of each individual corresponding wave mode from the cross-correlation analysis that is based on the separated wave mode out of a series of wave modes, through a filtering process of time series in the Fourier domain at locations y_1, y_2, and y_3.

4) Apply reverse Fourier transform to each individually separated wave mode through a filtering process of time series in the Fourier domain to the time domain, and obtain the amplitude of each mode of slosh waves.

5) Compute the value of $Max(A/\lambda)$ ratio for each mode of slosh waves from items 3 and 4.

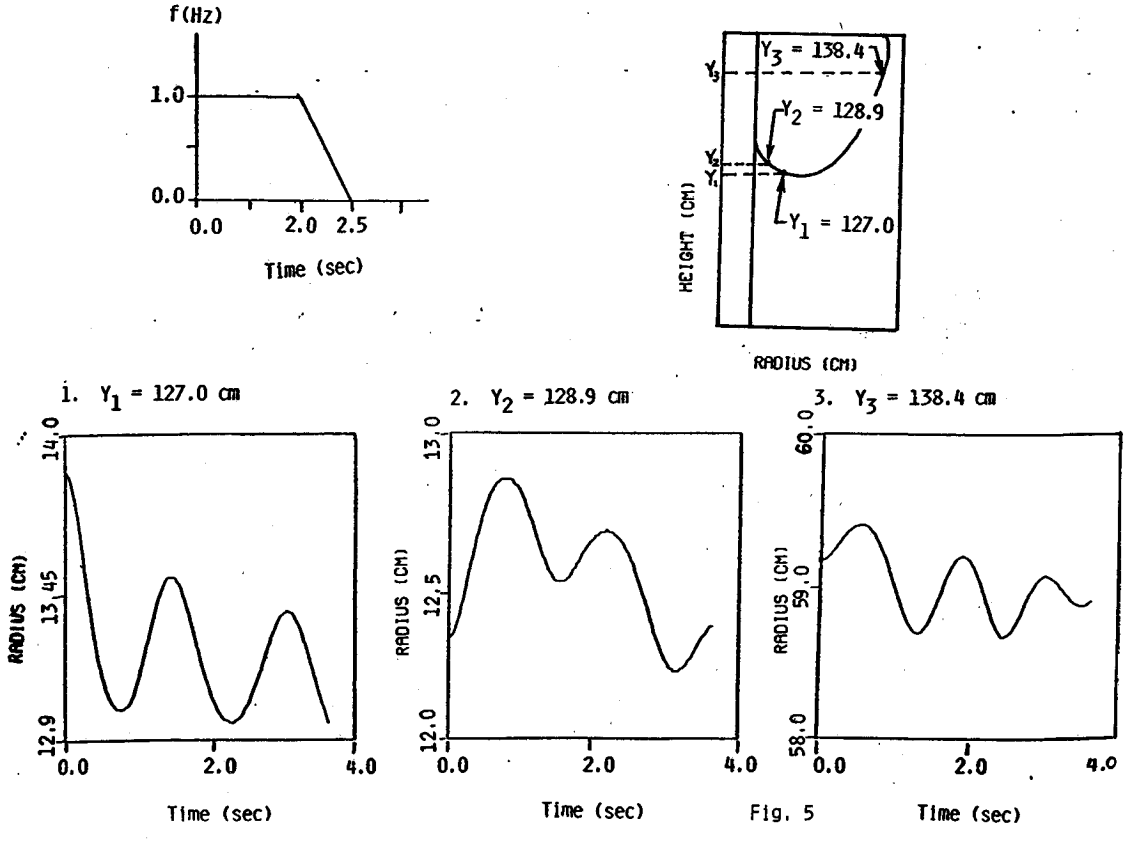

Fig. 5 Time series of wave amplitude fluctuations for the interface between liquid helium and helium vapor in a rotating dewar. The three time series shown are detected for interface at y_1 = 127.0 cm, y_2 = 128.9 cm, and y_3 = 138.4 cm in a vertical axis.

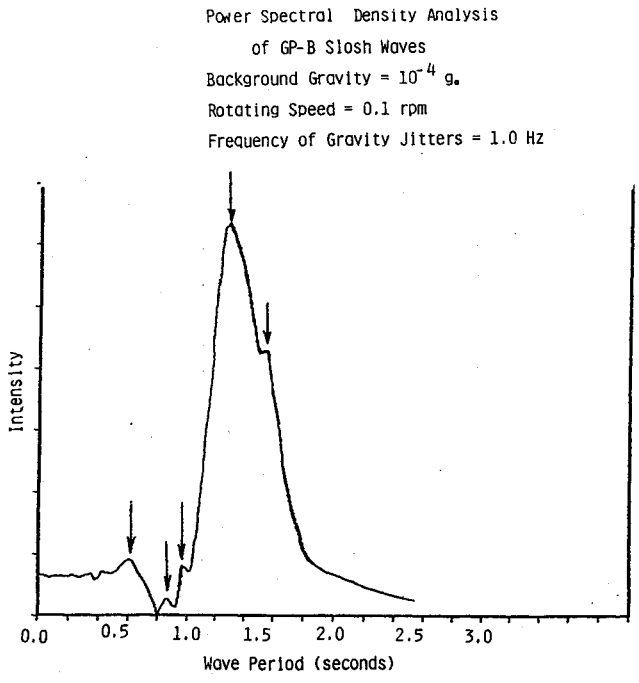

Fig. 6 Sample Fourier power spectral analysis of time series at y_1, shown in Fig. 4, indicating five major peaks of waves modes.

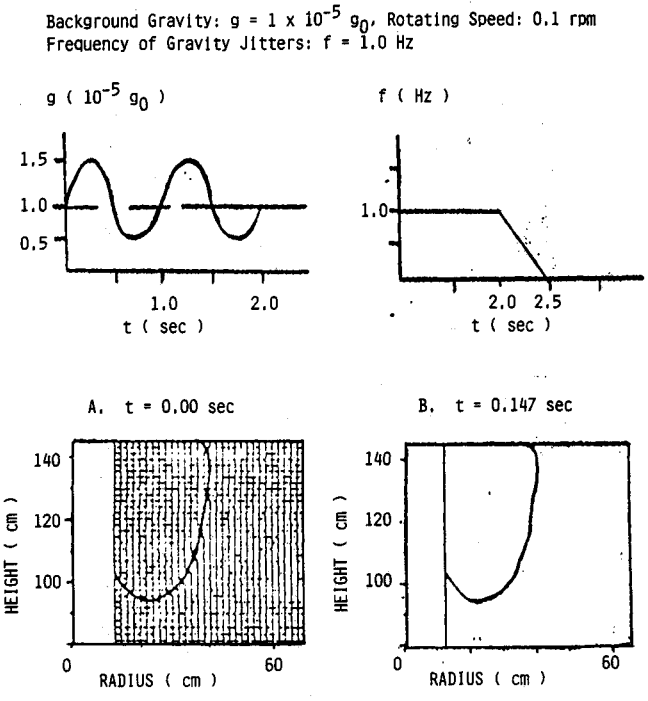

Figs. 7a and 7b Time sequence evolutions of interface between liquid helium and helium vapor in a rotating dewar (ω = 0.1 rpm) with a background gravity of 10^{-5} g_0, subjected to the vibration of gravity jitters with a frequency of 1.0 Hz. Top figures illustrate time-dependent variations of gravity environment and that of the frequency of gravity jitters. Figure 7a shows the profiles of interface at t = 0.0 s, and Fig. 7b at t = 0.147 s.

Figures 7a–7f show the evolution of slosh waves caused by gravity jitters and centrifugal force with a rotating speed of 0.1 rpm at the background gravity environment of 10^{-5} g_0. Again, top portions of Figs. 7a and 7b illustrate the variations of gravity environment with respect to time, and also the variations of gravity-jitter frequency with respect to time. Figures 7a–7f show time sequences of evolution for slosh waves from t = 0.0 to 3.42 s. Shown clearly is a series of slosh wave oscillations caused by gravity jitters and centrifugal

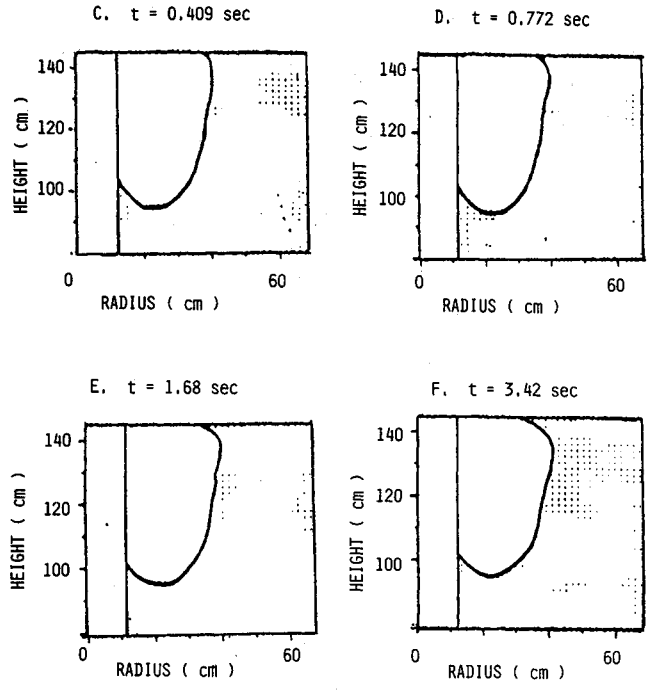

Figs. 7c–7f Time sequence evolutions of interface between liquid helium vapor in a rotating dewar (ω = 0.1 rpm) with a background gravity of 10^{-5} g_0, subjected to the vibration of gravity jitters with a frequency of 1.0 Hz. Figure 7c shows the profiles of interface at t = 0.409 s, Fig. 7d at t = 0.772 s, Fig. 7e at t = 1.68 s, and Fig. 7f at t = 3.42 s.

forces. Methods of data processing for the determination of wavelength, wave period, phase velocity, and propagation direction of slosh waves are similar to that described in the earlier case of the analysis of slosh waves induced by the gravity jitters at the background gravity environment of 10^{-4} g_0. Figure 8 shows a sample Fourier power spectral analysis for the present case. This figure clearly indicates that there are three major peaks of wave nodes corresponding to wave periods of 0.74, 1.22, and 1.46 s. A filter shall be properly chosen (by applying certain ranges of window for separating each wave mode out of three wave nodes contained in three time series, as described in the earlier case of analysis and shown in Fig. 5) for the determination of wavelength, phase velocity, and propagation direction of slosh waves.[22–25]

Table 2 shows the characteristics of major slosh waves induced by the restoring force field of gravity jitters and centrifugal forces. Analysis shows that there are two longitudinal modes and one transverse mode detected in this case. As indicated earlier, the existence of a transverse slosh mode is the production by the partially filled liquid contained in a special geometry rotating cylinder with the form of dewar-shaped cross section. Wave periods of longitudinal modes are 1.22 and 1.46 s, that of the transverse mode, 0.74 s. Again, the propagation direction is measured clockwise from positive axial direction. The value of $Max(A/\lambda)$ ratio for each slosh wave is calculated based on similar procedures discussed in an earlier study with background gravity level at 10^{-4} g_0, shown in Table 1.

Comparison between Tables 1 and 2 of the characteristics of slosh waves induced by the restoring force field of gravity jitters and centrifugal forces for different background gravity levels has been made. Conclusions may be drawn as follows:

1) Slosh waves of both longitudinal and transverse modes are excited in such a way that the geometry of a dewar-shaped rotating cylinder is responsible for the initiation of transverse modes, which are induced by the restoring force field of gravity jitters combined with centrifugal forces.

2) The longest wave period slosh waves, regardless of longitudinal or transverse modes, are responsible for the pro-

Table 1 Characteristics of major slosh waves in Gravity Probe-B Spacecraft experiment[a]

Type of wave mode	Wave period, s	Wavelength, cm	Phase velocity, cm/s	Propagation direction (clockwise from positive axial direction)	Ratio of maximum wave amplitude to wavelength [$Max(A/\lambda)$ ratio] (10^{-2})	Location of wave source
Longitudinal	1.46	84.86	58.30	193.98	0.6052	from top
Transverse	0.59	23.44	39.92	101.55	2.093	from left
	0.83	61.19	73.44	94.91	0.8016	from left
	1.03	39.95	38.94	94.44	1.2228	from left
	1.28	10.04	7.83	98.72	4.885	from left

[a]Background gravity: 10^{-4} g_0; rotating speed: 0.1 rpm; frequency of gravity jitters: 1.0 Hz.

Table 2 Characteristics of major slosh waves in Gravity Probe-B Spacecraft experiment[a]

Type of wave mode	Wave period, s	Wavelength, cm	Phase velocity, cm/s	Propagation direction (clockwise from positive axial direction)	Ratio of maximum wave amplitude to wavelength [$Max(A/\lambda)$ ratio] (10^{-2})	Location of wave source
Longitudinal	1.22	65.61	53.76	13.26	0.443	from bottom
	1.46	82.16	56.09	−9.01	0.993	from bottom
Transverse	0.74	13.67	11.20	−55.35	9.96	from right

[a]Background gravity: 10^{-5} g_0; rotating speed: 0.1 rpm; frequency of gravity jitters: 1.0 Hz.

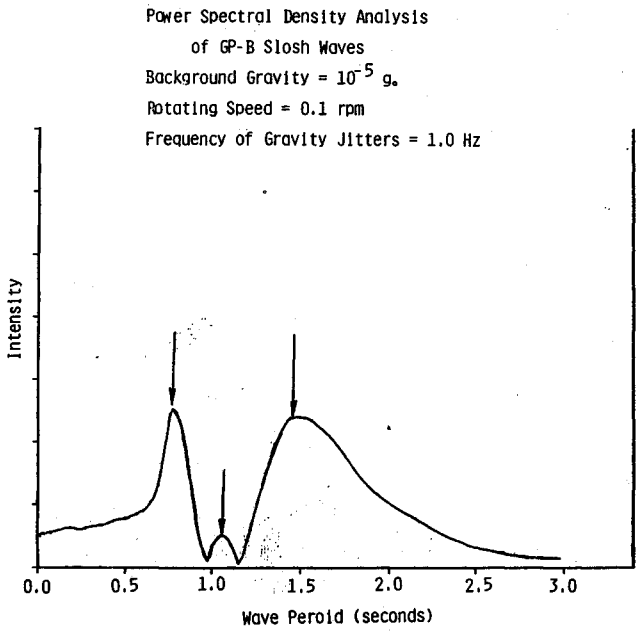

Fig. 8 Sample Fourier power spectral analylsis of time series for GP-B spacecraft slosh waves with $g = 10^{-5}$ g_0, $\omega = 0.1$ rpm, and $f_o = 1.0$ Hz, indicating three major peaks of wave modes.

duction of wave modes with the highest value of $Max(A/\lambda)$, compared to corresponding types of wave modes.

3) Slosh waves of the longest wave period transverse mode produce the wave mode with the highest value of $Max(A/\lambda)$, compared to that of the wave mode associated with the longitudinal mode slosh waves.

4) The square of the wave amplitude is proportional to the wave energy, which means that the lower frequency slosh waves have a higher wave energy than that of the higher frequency slosh waves.

5) Gravity jitters under a lower background gravity environment excite slosh waves with a higher value of $Max(A/\lambda)$, compared to that of the wave mode excited by gravity jitters under a higher background gravity environment.

Excitation of Slosh Waves due to Gravity Jitters at Different Rotating Speeds

The background gravity environment is 10^{-4} g_0; the frequency of gravity jitters is 1.0 Hz. Rotating speeds of the dewar cylinder at 0.1 and 1.0 rpm are considered, due to the fact that a spin rate of 1 rpm will be imposed for an instrument calibration in the early stages of the GP-B experiment, and a rotation rate of 0.1 rpm will be used during the normal operation for the GP-B spacecraft.

Figures 9a–9f show the evolution of slosh waves caused by gravity jitters and centrifugal forces, with a rotating speed of 1.0 rpm at the background gravity environment of 10^{-4} g_0. Top portions of Figs. 9a and 9b illustrate the variations of the gravity environment with respect to time, and also the variations of gravity-jitter frequency with respect to time. Figures 9a–9f show a time sequence of evolution for slosh waves from $t = 0.0$ to 3.03 s. Shown clearly is a series of slosh wave oscillations caused by the gravity jitters and centrifugal forces. Methods of data processing for the determination of wavelength, wave period, phase velocity, and propagation direction of slosh waves are similar to those described in the earlier case of the study of slosh waves induced by the gravity jitters and centrifugal forces, shown in Figs. 4–6. Figure 10 shows a sample Fourier power spectral analysis for the present case. This figure clearly indicates that there are three major peaks of wave modes corresponding to wave periods of 0.50, 0.92, and 1.22 s. Again, a filter shall be properly chosen (by applying certain ranges of window for separating each wave mode out of three wave nodes contained in three time series, as described in the earlier case of analysis and shown in Fig. 5) for the determination of wavelength, phase velocity, and propagation direction of slosh waves.[22–25]

Table 3 shows the characteristics of major slosh waves induced by the restoring force field of gravity jitters and centrifugal forces. Analysis shows that there are two longitudinal modes and one transverse mode detected in this case. As we indicated earlier, the existence of a transverse slosh mode is the production by the partially filled liquid contained in a special geometry rotating cylinder with the form of dewar-shaped cross-section. Wave periods of longitudinal modes are 0.92 and 1.22 s, that of the transverse mode is 0.50 s. Again, the propagation direction is measured clockwise from a positive axial direction. The value of $Max(A/\lambda)$ ratio for each

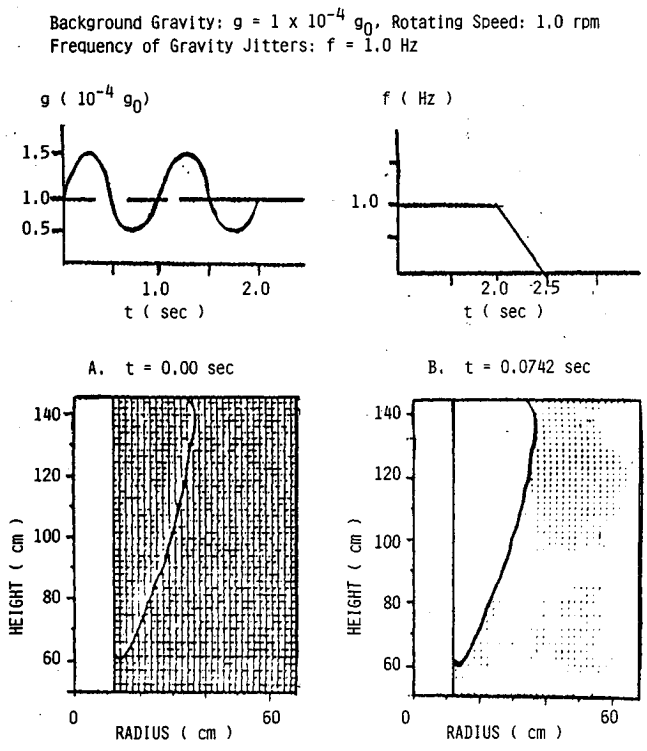

Figs. 9a and 9b Time sequence evolutions of interface between liquid helium and helium vapor in a rotating dewar (ω = 1.0 rpm) with a background gravity of 10^{-4} g_0, subjected to the vibration of gravity jitters with a frequency of 1.0 Hz. Top figures illustrate time-dependent variations of gravity environment and that of the frequency of gravity jitters. Figure 9a shows the profiles of interface at t = 0.0 s and Fig. 9b at t = 0.0742 s.

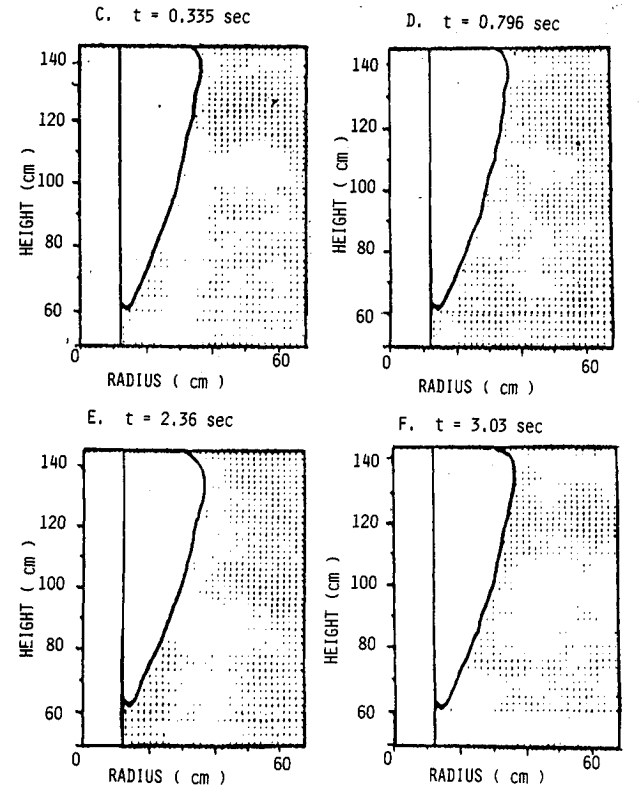

Figs. 9c–9f Time sequence evolutions of interface between liquid helium and helium vapor in a rotating dewar (ω = 1.0 rpm) with a background gravity of 10^{-4} g_0, subjected to the vibration of gravity jitters with a frequency of 1.0 Hz. Figure 9c shows the profiles of interface at t = 0.335 s, Fig. 9d at t = 0.796 s, Fig. 9c at t = 2.36 s, and Fig. 9f at t = 3.03 s.

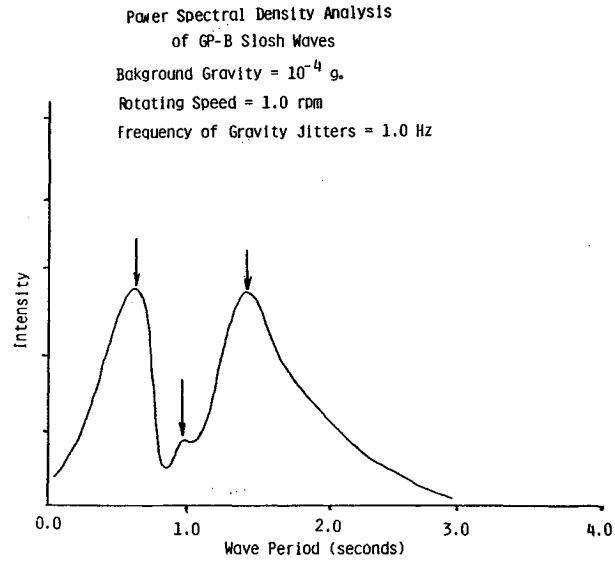

Fig. 10 Sample Fourier power spectral analysis of time series for GP-B spacecraft slosh waves with $g = 10^{-4}$ g_0, ω = 1.0 rpm, and f_o = 1.0 Hz, indicating three major peaks of wave modes.

slosh wave is calculated based on the procedures discussed in our earlier case of study, shown in Table 1.

To study the characteristics of slosh waves induced by gravity jitters at different rotating speeds of 0.1 and 1.0 rpm, comparisons between Tables 1 and 3 are made. We may draw the following conclusions:

1) Conclusions drawn for the study of case, shown in Table 1, in this paper stand.

2) Slosh waves induced by gravity jitters of partially filled liquid in a dewar with lower rotating speeds produce longer wave period transverse modes with a higher value of $Max(A/\lambda)$ ratio wave modes than that of slosh waves induced by gravity jitters in a dewar with higher rotating speed.

3) Higher centrifugal force and gravitational force tend to suppress the excitation of higher intensity slosh waves for partially filled liquid in a rotating dewar.

Discussion and Conclusions

The dynamical behavior of fluids, in particular, the effect of surface tension on partially filled fluids in a rotating dewar under microgravity environment, have been carried out by numerically computing the Navier-Stokes equations subjected to initial and boundary conditions. At the interface between the liquid and gaseous fluids, both the kinematic surface boundary condition and the interface stress conditions have been applied. The initial condition of bubble profiles was adopted from the steady-state formulations, in which the computer algorithms have been developed by Hung et al.[5,15] in a geometry of rotating dewar for the GP-B spacecraft.

Time evolution of slosh waves excited by the gravity jitters and centrifugal forces has been studied. Results show there is a group of wave trains, both in longitudinal and transverse modes, with various frequencies and wavelengths of slosh waves generated by the restoring force field of gravity jitters and centrifugal forces in this study. The longest wave periods of slosh waves, regardless of longitudinal or transverse modes, are responsible for the production of wave modes with the highest value of $Max(A/\lambda)$ ratio for the corresponding types of wave modes. Between longitudinal slosh waves and transverse slosh waves, the longest wave period transverse modes produce a greater value of $Max(A/\lambda)$ ratio wave mode than that of the wave mode associated with longitudinal slosh waves. Also, higher centrifugal force and gravitational force tend to suppress the excitation of higher intensity slosh waves.

Any fluid capable of motion relative to the spacecraft will be subject to an acceleration relative to the mass center of the

Table 3 Characteristics of major slosh waves in Gravity Probe-B Spacecraft experiment[a]

Type of wave mode	Wave period, s	Wavelength, cm	Phase velocity, cm/s	Propagation direction (clockwise from positive axial direction)	Ratio of maximum wave amplitude to wavelength [$Max(A/\lambda)$ ratio] (10^{-2})	Location of wave source
Longitudinal	0.92	129.01	140.65	162.66	1.47	from top
	1.22	86.66	71.22	142.64	1.74	from top
Transverse	0.50	11.02	22.10	−36.55	3.83	from right

[a]Background gravity: 10^{-4} g_0; rotating speed: 1.0 rpm; frequency of gravity jitters: 1.0 Hz.

spacecraft arising from the gravity gradient of the Earth.[27-29] In addition to the Earth's gravitational force, the interaction between the particle mass of fluids and the spacecraft mass due to gravity gradient accelerations[28] has been considered in the present study.

In this study, we have demonstrated that the computer algorithm presented, through the execution of supercomputer CRAY X-MP, can be used to simulate the fluid behavior in a microgravity environment, in particular, the excitation of slosh waves due to different gravity environments and rotating speeds, and to provide information on the characteristics of the cryogenic liquid propellant (subjected to possible gravity jitters) to be used in the GP-B spacecraft propulsion and, also, in the dewar-shaped propellent container.

Acknowledgment

The authors appreciate the support received from NASA through Grants NAG8-035, NAG8-129, and NAGW-812. They would like to express their gratitude, also, to Richard A. Potter of NASA/Marshall Space Flight Center for the stimulating discussions during the course of the present study.

References

[1]Wilkinson, D. T., Bender, P. L., Eardley, D. M., Gaisser, T. K., Hartle, J. B., Israel, M. H., Jones, L. W., Partridge, R. B., Schramm, D. N., Shapiro, I. I., Vessort, R. F. C., and Wagoner, R. V., "Gravitation, Cosmology and Cosmic-Ray Physics," *Phys. Today*, Vol. 39, 1986, pp. 43–46.

[2]"Stanford Relativity Gyroscope Experiment (NASA Gravity Probe B)," *Proceedings of Society of Photo-Optical Instrumentation Engineers*, Vol. 619, Society of Photo-Optical Instrumentation Engineers, Bellingham, WA, 1986, pp. 1–165.

[3]Schafer, C. F., and Lowry, S. A., "Mechanics of Liquid Helium in a Partially Filled Rotating Dewar in Low Gravity—With Application to Gravity Probe-B," *NASA TP-2124*, Jan. 1983, pp. 38.

[4]Hung, R. J., and Leslie, F. W., "Bubble Shapes in a Liquid-Filled Rotating Container Under Low Gravity," *Journal of Spacecraft and Rockets*, Vol. 25, 1988, pp. 70–74.

[5]Hung, R. J., Tsao, Y. D., Hong, B. B., and Leslie, F. W., "Bubble Behaviors in a Slowly Rotating Helium Dewar in Gravity Probe-B Spacecraft Experiment," *Journal of Spacecraft and Rockets*, Vol. 26, 1988, pp. 167–172.

[6]Hung, R. J., Tsao, Y. D., Hong, B. B., and Leslie, F. W., "Dynamical Behavior of Surface Tension on Rotating Fluids in Low and Microgravity Environments," *International Journal for Microgravity Research and Applications*, Vol. 11, 1989, pp. 81–95.

[7]Leslie, F. W., "Measurements of Rotating Bubble Shapes in a Low Gravity Environment," *Journal of Fluid Mechanics*, Vol. 161, 1985, pp. 269–279.

[8]Kitchens, C. W., Jr., "Navier-Stokes Equations for Spin-Up in a Filled Cylinder," *AIAA Journal*, Vol. 18, No. 8, 1980, pp. 929–934.

[9]Veldman, A. E. P., and Vogels, M. E. S., "Axisymmetric Liquid Sloshing Under Low Gravity Conditions," *Acta Astronautica*, Vol. 11, 1984, pp. 641–649.

[10]Homicz, G. F., and Gerber, N., "Numerical Model for Fluid Spin-Up from Rest in a Partially Filled Cylinder," *Journal of Fluids Engineering*, Vol. 109, 1987, pp. 194–197.

[11]Kamotani, Y., Prasad, A., and Oastrach, S., "Thermal Convections in an Enclosure due to Vibrations Aboard a Spacecraft," *AIAA Journal*, Vol. 19, 1981, pp. 511–516.

[12]*Technology for Future NASA Missions: Civil Space Technology Initiative and Pathfinder*, NASA Office of Aeronautics and Space Technology, NASA CP-3016, 1988, p. 568.

[13]Hung, R. J., Lee, C. C., and Shyu, K. L., "Reorientation of Rotating Fluid in Microgravity Environment With and Without Gravity Jitters," *Journal of Spacecraft and Rockets*, Vol. 28, 1991 pp. 71–78.

[14]Hung, R. J., Tsao, Y. D., Hong, B. B., and Leslie, F. W., "Time Dependent Dynamical Behavior of Surface Tension on Rotating Fluids under Microgravity Environment," *Advances in Space Research*, Vol. 8, No. 12, 1989, pp. 205–213.

[15]Hung, R. J., Tsao, Y. D., Hong, B. B., and Leslie, F. W., "Axisymmetric Bubble Profiles in a Slowly Rotating Helium Dewar Under Low and Microgravity Environments," *Acta Astronautica*, Vol. 19, 1989, pp. 411–426.

[16]Mason, P., Collins, D., Petrac, D., Yang, L., Edeskuty, F., Schuch, A., and Williamson, K., "The Behavior of Superfluid Helium in Zero Gravity," *Proceedings of 7th International Cryogenic Engineering Conference*, Science and Technology Press, Surrey, England, UK, 1978.

[17]Hung, R. J., "Superfluid and Normal Fluid Helium II in a Rotating Tank Under Low and Microgravity Environments," *Proceedings of National Science Council, Series (A)*, Vol. 14, Taipei, Taiwan, 1990, pp. 289–297.

[18]Harlow, F. H., and Welch, J. E., "Numerical Calculation of Time-Dependent Viscous Incompressible Flow of Fluid with Free Surface," *Phys. Fluids*, Vol. 8, 1965, pp. 2182–2189.

[19]Spalding, D. B., "A Novel Finite-Difference Formulation for Differential Expressions Involving Both First and Second Derivatives," *International Journal of Numerical Methods in Engineering*, Vol. 4, 1972, pp. 551–559.

[20]Patankar, S. V., *Numerical Heat Transfer and Fluid Flow*, Hemisphere-McGraw-Hill, NY, 1980, p. 197.

[21]Patankar, S. V., and Spalding, D. B., "A Calculation Procedure for Heat, Mass and Momentum Transfer in Three Dimensional Parabolic Flows," *International Journal of Heat and Mass Transfer*, Vol. 15, 1972, pp. 1787–1805.

[22]Hung, R. J., Phan, T., and Smith, R. E., "Observation of Gravity Waves During the Extreme Tornado Outbreak of April 3, 1974," *Journal of Atmospheric and Terrestrial Physics*, Vol. 40, 1978, pp. 831–843.

[23]Hung, R. J., and Smith, R. E., "Ray Tracing of Gravity Waves as a Possible Warning System for Tornadic Storms and Hurricanes," *Journal of Applied Meteorology*, Vol. 17, 1978, pp. 3–11.

[24]Hung, R. J., and Kuo, J. P., "Ionospheric Observation of Gravity Waves Associated with Hurricane Eloise," *Journal of Geophysics*, Vol. 45, 1978, pp. 67–80.

[25]Hung, R. J., Phan, T., and Smith, R. E., "Coupling of Ionosphere and Troposphere During the Occurrence of Isolated Tornados of November 20, 1973," *Journal of Geophysical Research*, Vol. 84, 1979, pp. 1261–1268.

[26]Hung, R. J., Lee, C. C., and Leslie, F. W., "Effect of G-Jitters on the Stability of Rotating Bubble Under Microgravity Environment," *Acta Astronautica*, Vol. 21, 1990, pp. 309–321.

[27]Forward, R. L., "Flattering Space-Time Near the Earth, "*Physical Review, D*, Vol. 26, 1982, p. 735.

[28]Misner, C. W., Thorne, K. S., and Wheeler, J. A., *Gravitation*, W. H. Freeman and Co., 1973, p. 1279.

[29]Avduyevsky, V. S., ed, *Scientific Foundations of Space Manufacturing*, MIR Publishing Co., Moscow, USSR, 1984.